Beyond the Desert: Tevatron and LHC Results on Searches for Physics Beyond the Standard Model

G. Redlinger
Physics Department, Brookhaven National Laboratory, Upton, NY, USA

arXiv:1109.6927v1 [hep-ex] 30 Sep 2011

This is a brief and limited review of searches for physics beyond the Standard Model from the ATLAS,CDF,CMS and D0 experiments, as of the end of July 2011. Priority is given to the most recent results and to those with the largest integrated luminosity analyzed.

1. Introduction

As the searches for physics beyond the Standard Model (SM) at the LHC get fully underway this year, the desert is on the minds of many people. The desert has special meaning in particle physics of course, representing perhaps our greatest hope and our greatest fear. The hope is that we discover new physics at the LHC, and that this new physics holds in the desert scenario all the way up to the GUT scale. The fear is that we discover nothing, a fear echoed by Bob Park in his widely read "What's New" column where, on the occasion of the first major release of results from the LHC experiments, he reminisces about the look on Carl Sagan's face 32 years ago when the first Mars lander sent back desolate images of the Martian desert [1].

Given the large number of search results from the Tevatron and LHC experiments, a comprehensive review is beyond the scope of this document, and some selection/organizing principle is needed. There is a temptation to organize by theoretical concepts, but this violates the spirit of Beyond SM (BSM) searches which are typically signature based and not tied to specific models.[1] However, a full review of all possible experimental signatures is also beyond the scope of this note.

The note is therefore organized as follows. For the Tevatron searches, after a brief listing of the most recent results from a rich program, the focus will instead be on two of the "anomalies" that have caught the attention of the community recently. This is followed by a review of the most recent LHC results up to the end of July, where priority is given to the most recent results with the largest integrated luminosity analyzed. A full listing of all analyses can be found at [2]. The reader should also consult [3] and [4] from this conference for other search results involving heavy flavor (i.e. bottom and charm) and top quarks, respectively.

2. Results from the Tevatron

At the Tevatron, about 11.5 fb^{-1} have been delivered to each experiment and a little over 10 fb^{-1} recorded. Recent search results from CDF and D0 involve 5-6 fb^{-1} of data, although some go as high as 9 fb^{-1}. Tables I and II summarize some of the most recent BSM searches from D0 and CDF. Among the noteworthy new results are: *i)* the diphoton resonance search by CDF [5] which, combined with results from dilepton resonances, set a new limit on Randall-Sundrum gravitons, *ii)* a long-lived charged particle search from D0 [6] which set new limits on higgsino-like and gaugino-like charginos, and *iii)* the anomaly in the D0 like-sign dimuon charge asymmetry measurement [7] where a 3.9σ deviation from SM expectations was seen.

Other sightings at the Tevatron that have caught the attention of the community recently are the peak in the dijet mass spectrum in W+2jets events and the forward-backward asymmetry in $t\overline{t}$ production.

2.1. Dijet mass spectrum in W+2jets events

CDF reported earlier this year [25] on an excess in the dijet mass spectrum in the 120-160 GeV range based on an analysis of 4.3 fb^{-1} of data. The analysis has been recently extended [26] to 7.3 fb^{-1}. Using the same analysis cuts and strategy, the excess in the dijet mass distribution, shown in Fig. 1(left), increases from 3.2σ to 4.1σ. The estimated cross section of the excess is 3.0 ± 0.7 pb, assuming the acceptance follows that of W+Higgs production.

[1] Although most analyses do include interpretations in one or more models.

Table I: Incomplete summary of some of the most recent BSM searches from D0.

Signature	$\int \mathcal{L}dt$ (fb^{-1})	**Ref.**	**Comment**
long-lived slow particle	5.2	[6]	M > 230 (251) GeV for higgsino(gaugino)-like chargino
dimuon asymmetry	9	[7]	3.9σ deviation from SM
W' $\rightarrow$ tb	2.3	[8]	M(W') > 863 GeV
WW/WZ resonance	5.4	[9]	M(RS graviton) > 300-754 GeV
$e\nu jj$ resonance	5.4	[10]	M(LQ(1)) > 326 GeV ($BR = 0.5$)
$t' \rightarrow qW$	5.3	[11]	M(t') > 285 GeV (2.5σ excess in μ channel)
$\gamma\gamma + E_T^{miss}$	6.3	[12]	$\Lambda > 124$ TeV (minimal GMSB)
$\tilde{t} \rightarrow bl\tilde{\nu}(l = e, \mu)$	5.4	[13]	M($\tilde{t}$) > 210 GeV for M($\tilde{\nu}$) < 110 GeV

Table II: Incomplete summary of some of the most recent BSM searches from CDF.

Signature	$\int \mathcal{L}dt$ (fb^{-1})	**Ref.**	**Comment**
$\gamma\gamma$ resonance	5.7	[14]	M(RS graviton) > 1111 GeV, (ee,$\mu\mu$,$\gamma\gamma$ combined, $k/\overline{M}_{pl} = 0.1$)
ZZ resonance ($ll\nu\nu$,$llll$,$lljj$)	6	[15]	M(RS graviton) > $\sim$ 600 GeV
$l + \gamma + E_T^{miss}$ + bjet (also $t\bar{t} + \gamma$)	6	[16]	$\sigma(t\bar{t} + \gamma) = 0.18 \pm 0.07$ pb
jjj resonance	3.2	[17]	cross section limits vs mass for RPV gluino
$t' \rightarrow b + W$	5.6	[18]	M(t') > 358 GeV
$b' \rightarrow t + W$	4.8	[19]	M(b') > 372 GeV
$t' \rightarrow t + E_T^{miss}$	5.7	[20]	M(t') > 400 GeV for M(inv) < 70 GeV
$t\bar{t}$ resonance	4.8	[21]	M(Z') > 900 GeV
$ZZ + E_T^{miss}$	4	[22]	$\sigma > 300$ fb
same-sign dilepton	6.1	[23]	consistent with SM
bbb resonance	2.6	[24]	σ limits as function of mass

D0 [27] does not confirm the excess, following the same analysis methods on 4.3 fb^{-1} of data. Accordingly, limits are set on the production cross section, shown in Fig. 1(middle), excluding the original crude estimate by CDF of the cross section of 4 pb^{-1} by a significant margin. However, the situation is a little bit more ambiguous now, given the most recent estimate of the cross section from CDF. There had also been some worry that the Monte Carlo tuning done by D0 would have erased the effect, but it has been shown that these correction factors have very little effect. ATLAS [28] has also made a search in their W+2jets data. They too come up empty; the ATLAS mass spectrum in W+2jets events is shown in Fig. 1(right).

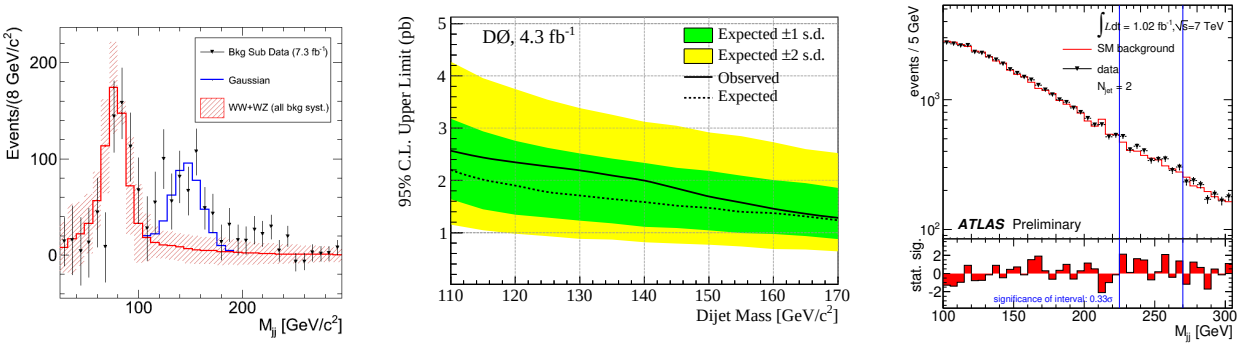


Figure 1: Left: Dijet mass spectrum in W+2jet events from CDF [26]. Center: D0 limits on the cross section for an excess as a function of the dijet mass [27]. Right: Dijet mass spectrum in W+2jet events from ATLAS [28].

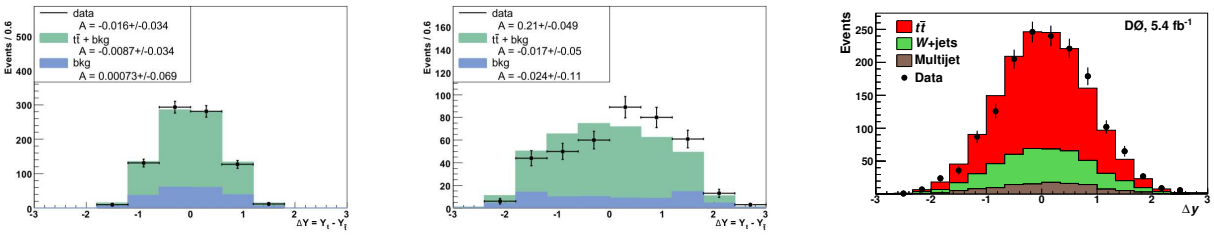


Figure 2: Left and Center: Distributions of Δy in $t\bar{t}$ events from CDF [29] in the lepton+jets channel. Left: for $M(t\bar{t}) < 450$ GeV. Center: for $M(t\bar{t}) > 450$ GeV. Right: Distribution of Δy from D0 [32] in the lepton+jets channel.

2.2. $t\bar{t}$ forward-backward asymmetry

Turning to $t\bar{t}$ production, CDF [29] has compared the production rate in the forward and backward hemispheres with 5.3 fb^{-1} of data. A small asymmetry is expected in the SM from interference between leading-order and next-to-leading order diagramss. CDF first observed an asymmetry in the lepton+jets channel; the effect is particularly enhanced at large values of the mass of the $t\bar{t}$ pair and also at large values of the rapidity difference between t and $\bar{t}$. Fig. 2 (left) shows the distribution of Δy for $M(t\bar{t}) < 450$ GeV while Fig. 2 (center) shows the distribution for $M(t\bar{t}) > 450$ GeV. The asymmetry, corrected back to parton level and evaluated in the $t\bar{t}$ rest frame is $A^{t\bar{t}} = 0.475 \pm 0.114$ for $M(t\bar{t}) > 450$ GeV, to be compared with the prediction using MCFM [30], $A^{t\bar{t}} = 0.088 \pm 0.013$, amounting to a 3.4σ discrepancy.

More recently, CDF has studied the dileptonic $t\bar{t}$ channel [31] and found a 2.3σ deviation, $A^{t\bar{t}} = 0.42 \pm 0.15(\text{stat}) \pm 0.05(\text{sys})$, again for $M(t\bar{t}) > 450$ GeV. D0 has analyzed the lepton+jets channel with 5.4 fb^{-1} of data [32]. They measure the asymmetry in two ways, based on Δy and also a simpler analysis based on the lepton direction. They also observe an asymmetry significantly above SM expectations, but no particular enhancement at large Δy or at large $M(t\bar{t})$. Whether this is a sign of New Physics or points to a deficiency in higher-order QCD calculations remains an open question. As pointed out by D0, some Monte Carlo generators predict a dependence of the asymmetry on the p_T of the $t\bar{t}$ system. They find that their measurement of $p_T(t\bar{t})$ comes out softer than Monte Carlo predictions, which would lead to a larger asymmetry predicted in the SM.

Due to the fact that the LHC is a proton-proton machine, there is no forward-backward asymmetry. However, the rapidity distribution of top quarks is broader than that of anti-top quarks due to the difference in momentum fraction carried by initial-state quarks versus anti-quarks. Since the charge asymmetry arises from a next-to-leading-order effect in quark-antiquark annihilation, while $t\bar{t}$ pairs are produced at the LHC mainly by gluon fusion, the predicted asymmetry is even smaller at the LHC than at the Tevatron. First measurements from ATLAS [33] with 0.7 fb^{-1} and CMS [34] with 1.09 fb^{-1} come out consistent with the SM but still with large uncertainties.

3. Results from the LHC

As of the end of July, around the time of this conference, ATLAS and CMS have each collected about 1.5 fb^{-1} of data at 7 TeV. The LHC is running very well, reaching a peak luminosity of about 2×10^{33} as of the end of July 2011. Both ATLAS and CMS have produced search results with about 1 fb^{-1} analyzed.

3.1. Searches for resonances

We start with the most classic of new physics searches, the dilepton resonance, looking for bumps in the mass spectrum of isolated high p_T opposite-sign, same-flavor leptons [35, 36]. ATLAS and CMS have updated their previous searches to approximately 1.1 fb^{-1}. The lepton p_T and η cuts are roughly the same in the two experiments. The background is dominated by the Z-pole and continuum Drell-Yan production, and is estimated from Monte Carlo. As an example, the dielectron invariant mass distribution from ATLAS is shown in Fig. 3 (left). No significant deviation from expectations is seen in either experiment, and limits are set on a number of Z' models. One standard benchmark is the sequential standard model (SSM) Z' which has the same

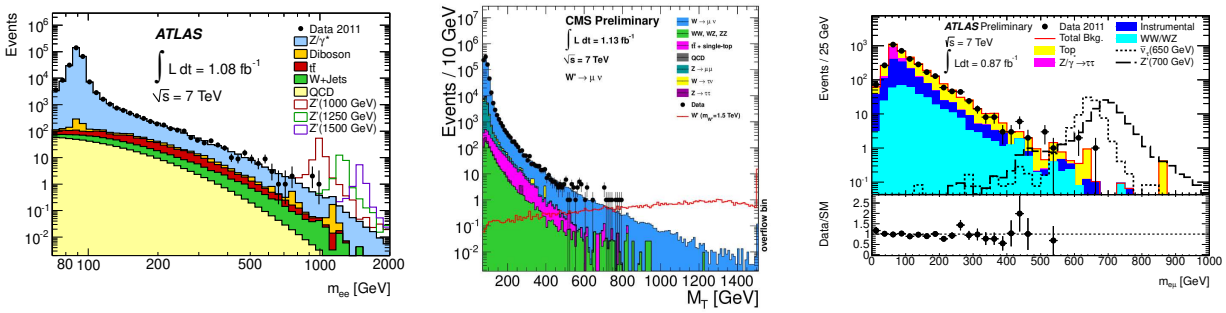


Figure 3: Left: Dielectron invariant mass from ATLAS [35]. Center: transverse mass between E_T^{miss} and the muon from CMS [38]. Right: $e^{\pm}\mu^{\mp}$ invariant mass from ATLAS [39].

couplings and decays as the SM Z but is heavier. Both ATLAS and CMS set a limit[2] of close to 2 TeV on the SSM Z' mass, from combining ee and $\mu\mu$ channels and now surpass the limits from the Tevatron. Limits on other Z' and Randall-Sundrum graviton models have also been produced that exceed limits from the Tevatron.

ATLAS and CMS have updated their searches for peaks in the transverse mass (M_T) spectrum of events with a high p_T lepton and missing transverse momentum (E_T^{miss}) [37, 38]. The main background comes from the tail of the SM W. This is estimated by Monte Carlo in the case of ATLAS. CMS makes a fit to the low M_T region and extrapolates to higher M_T. The transverse mass distribution from CMS in the muon channel is shown in Fig. 3 (center). ATLAS and CMS set comparable limits of about 2.2 TeV, combining electron- and muon-channels. This represents an improvement by about 50%, or approximately 700 GeV, in the mass limit, for an approximately 30-fold increase in the integrated luminosity, going from the previous result based on 35 pb^{-1} to the current 1 fb^{-1}.

ATLAS has also searched for a resonance in isolated $e\mu$ pairs [39]. The invariant mass distribution is shown in Fig. 3 (right) where it can be seen that the main background sources are $t\bar{t}$ and jet instrumental background where a jet from either W/Z+jets or QCD multijet events fakes a lepton. Monte Carlo is used to estimate the $t\bar{t}$ background. The jet background is estimated using the standard matrix method. In order to take into account the dependence of the fake rate on the event kinematics, the matrix equation is solved event by event for a set of weights; these weights are then summed over all events. Limits are set on the cross section (σ) times branching ratio (BR), using a R-parity violating model with a tau sneutrino ($\tilde{\nu}_\tau$) decaying to $e+\mu$ to compute the acceptance ($\mathcal{A}$). Using the same model, limits are also set in the plane of the $\tilde{\nu}_\tau$ to $d\bar{d}$ coupling λ'_{311} as a function of the $\tilde{\nu}_\tau$ mass, for various values of the coupling λ_{312} of $\tilde{\nu}_\tau$ to $e\mu$. ATLAS now supersedes the D0 limit [40] on the coupling for almost all masses, and improves significantly on the limit at high mass.

Another classic search is the hunt for a bump in the dijet mass spectrum; an example from ATLAS is shown in Fig. 4 (left). ATLAS uses the anti-k_t [41] jet algorithm with the distance parameter $R = 0.6$. CMS starts with anti-k_t jets with $R = 0.5$, selects the resulting two highest p_T jets and then adds other jets that were found within a radius of 1.1. Both ATLAS and CMS derive limits on $\sigma \times \mathcal{A}$ as a function of the resonance mass [42, 43]. Limits in a number of models have been derived. For example, both ATLAS and CMS set limits ranging from 2.7 to 3 TeV on excited quarks and on axigluon models. The ATLAS mass limits improve by approximately 30% in going from the previous results based on 35 pb^{-1} to the current results based on 0.81 fb^{-1}. Fig. 4 (center) shows model-independent limits from CMS on $\sigma \times \mathcal{A}$ for different subprocesses at parton level, assuming a narrow resonance; the plot on the right from ATLAS shows the dependence on the width of the resonance.

CMS has updated the search for $t\bar{t}$ resonances [44], in the all-hadronic channel, focusing on the case where the top quarks are sufficiently boosted such that some of the decay products may be merged; this signature is efficient only for $t\bar{t}$ masses above approximately 1 TeV. Two topologies are considered: i) a dijet topology in which all three jets from the top quark are merged, and ii) a 3-jet topology in which the decay products are completely merged in one hemisphere, while only the decay products of the W are merged in the other. Top quarks and W's are tagged by analyzing the jet substructure. The jet energy scale for merged jets is checked by examining the mass of the highest mass jet in the hadronic hemisphere of boosted semileptonic $t\bar{t}$ events. Fig. 5 (left) shows the position of the resulting W-mass peak. The background, dominated by QCD multijets,

[2]All limits in this document will be at 95% confidence level, unless otherwise stated.

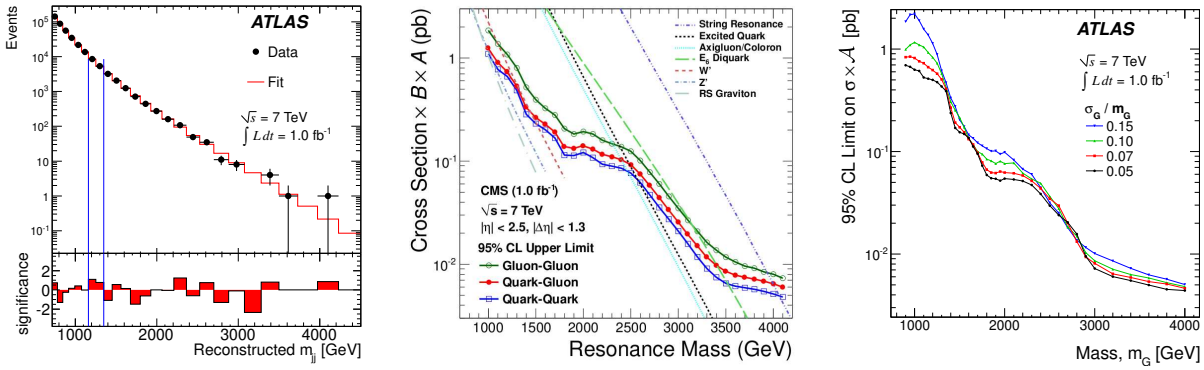


Figure 4: Left: Dijet invariant mass spectrum from ATLAS [42]. Center/right: Model-independent upper limits from CMS and ATLAS on $\sigma \times \mathcal{A}$ for dijet resonances. Center: For narrow-resonances, the dependence on the parton-level subprocess [43]. Right: The dependence on the resonance width [42].

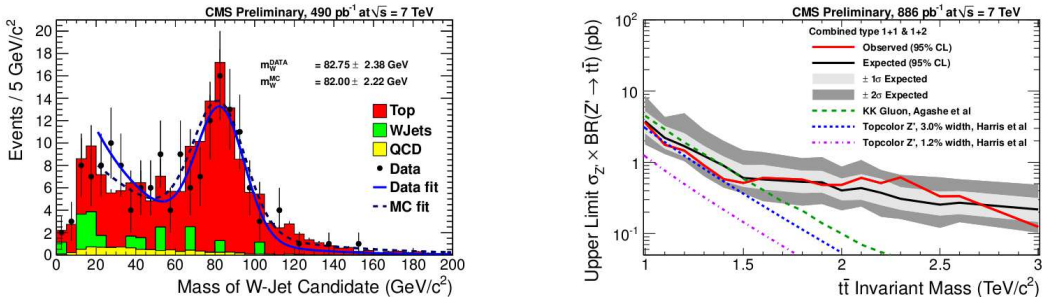


Figure 5: Left: Mass of the highest mass jet in the hadronic hemisphere of boosted semi=leptonic $t\bar{t}$ events. Right: Limits on $\sigma \times BR(Z' \to t\bar{t})$ from [44].

is estimated directly from the data, by selecting events with one top-tagged jet, and applying a top-mistag rate, also estimated from the data. The small background from $t\bar{t}$ is estimated via Monte Carlo. Limits are set on the production cross section times branching ratio for a $Z' \to t\bar{t}$, as shown in Fig. 5 (right).

3.2. Other searches

CMS has searched for a fourth-generation t' quark [45], assuming a decay to $W + b$. The search is done in the semi-leptonic channel, requiring one isolated lepton and four or more jets, at least one of which is b-tagged. A kinematic fit is performed to compute the t' mass, and the search is performed in the plane of H_T versus the fitted mass, where H_T is defined as the scalar sum of E_T^{miss} and the transverse energies of the lepton and jets. The main background comes from $t\bar{t}$ and to a lesser extent W+jets; all backgrounds are estimated using the Monte Carlo. Combining electron and muon channels, t' quarks are excluded below 450 GeV, surpassing the Tevatron limit.

ATLAS has updated the search for monojets and large E_T^{miss} [46]. Three signal regions are defined, with varying cuts on the leading jet p_T, E_T^{miss} and the veto thresholds for additional jets in the event. The dominant backgrounds from $Z(\to \nu\overline{\nu})$+jets and from $W(\to \ell\nu)$+jets are estimated using Monte Carlo normalized to a muon control sample (but with the requirements on jet p_T, E_T^{miss} and subleading jet vetoes the same as in the signal search) from the data. Multijet background is estimated by a linear extrapolation of the p_T of the subleading jet below the jet veto threshold, using a sample of events where E_T^{miss} points along the subleading jet direction. Fig. 6 (left) shows the resulting model-independent limits on $\sigma \times \mathcal{A}$. Limits are also set in the ADD large extra dimensions model on the $4 + n$-dimensional Planck scale (M_D) as a function of the number of extra dimensions. For the number of extra dimensions ranging from 2 to 6, M_D values between 3.2 TeV and 2.0 TeV are excluded as shown in Fig. 6 (right).

CMS has updated the search for microscopic black holes [47]. The main discriminating variables are: i) S_T, the scalar sum of the p_T of all jets, electrons, muons, photons and E_T^{miss} where each of the objects is required

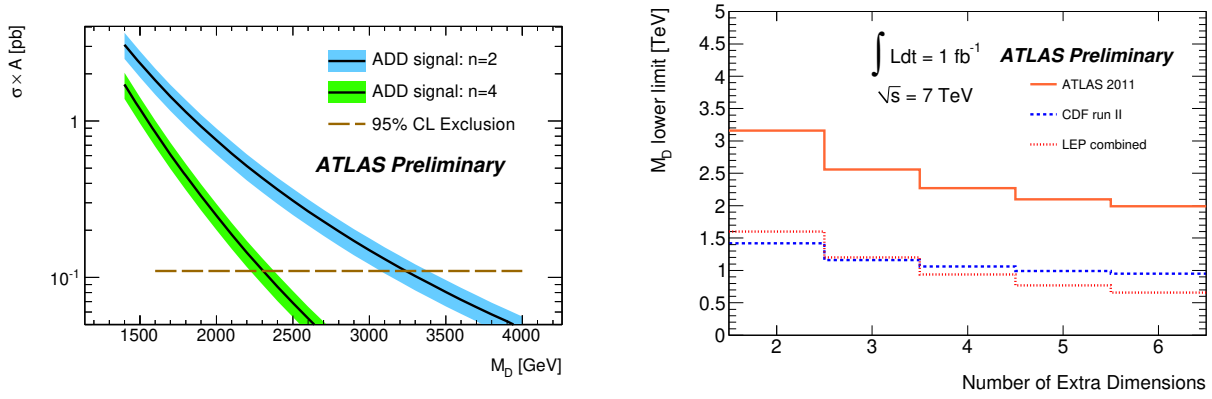


Figure 6: Left: Model-independent limit on $\sigma \times \mathcal{A}$ as a function of the $4+n$-dimensional Planck scale, M_D for 2 and 4 extra dimensions. Right: Limits on M_D as a function of the number of extra dimensions. From [46].

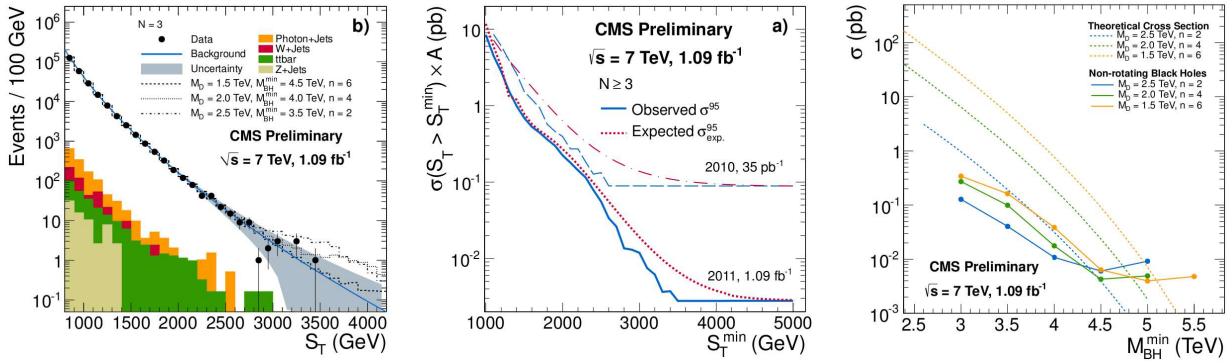


Figure 7: Left: Total transverse energy for events with $N = 3$ photons, electrons, muons or jets in the final state. Center: Model-independent limits on $\sigma \times \mathcal{A}$ for $S_T > S_T^{min}$ as a function of S_T^{min}, for events with 3 or more objects in the event. Righ: Cross section limits compared with signal production cross sections from the BLACKMAX generator. The colored solid lines show the experimental cross section limits, while the dotted lines sohw the corresponding signal cross sections. From [47].

to be greater than 50 GeV, and ii) N, the number of objects in the event. The main background of multijet and photon+jets events is estimated by exploiting the independence of the shape of the S_T distribution on the multiplicity of objects in the event; the S_T shape is determined for $N = 2$ where no signal is present, as verified in the dijet analysis. The distribution of S_T for $N = 3$ is shown in Fig. 7 (left). Limits are set on $\sigma \times \mathcal{A}$ for $S_T > S_T^{min}$, as shown in Fig. 7 (center) for $N \geq 3$. Limits are also set on black hole masses in the context of the BLACKMAX [48] model, as shown in Fig. 7 (right); black hole masses below approximately 4.5-5 TeV are excluded in this model.

3.3. Searches for slow-moving or stopped charged, massive particles

CMS has updated the search for slow-moving, massive, charged particles [49]. These arise quite generically in many SUSY models, for example. They make two types of measurements, tracker-only and tracker plus the muon system. An estimation of the mass comes from the track momentum and either the track dE/dx or the time-of-flight (TOF) to the muon system. The background is estimated via the commonly called "ABCD" method, exploting the lack of correlation between momentum, TOF and dE/dx. The resulting mass distribution from the combined analysis is shown in Fig. 8 (left). From the tracker only analysis, they set limits on stop R-hadrons and gluino R-hadrons, reaching limits close to 1 TeV for the gluino case, as shown in Fig. 8 (center). From the combined analysis, shown in Fig. 8 (right) they exclude the partners of the tau lepton (staus) in a minimal GMSB model (following SPS line 7 [50]), excluding masses below 293 GeV.

CMS has also updated the search for stopped gluino/stop R-hadrons [51]. They look for the R-hadron decay in the calorimeter in between bunches or during interfill periods. Potential background sources include detector

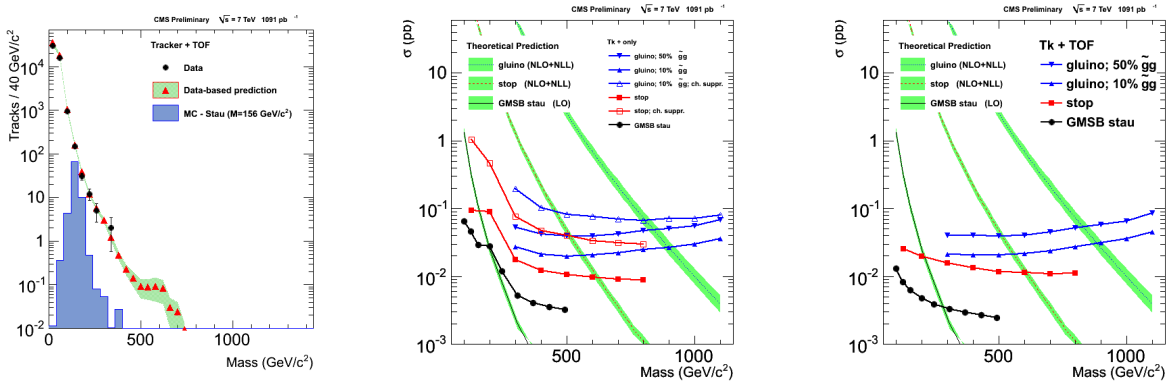


Figure 8: Left: Mass distribution from the combined analysis of tracker dE/dx and muon TOF [49]. Center/right: Theoretical cross sections and observed limits on the cross section for a variety of models. Center: tracker dE/dx analysis. Right: combined tracker dE/dx plus muon TOF analysis.

noise, beam-related background, and cosmics. These are estimated using 2010 data. Noise and cosmics rates were measured when the LHC luminosity was around 10^{28} cm^{-2}sec^{-1}. The rate from beam background and noise+cosmics was estimated from the rest of the 2010 run. Given vastly different beam conditions in 2011 and potentially different detector conditions, this background estimation might be subject to some uncertainty, but in the end the CMS observations match expectations over a wide range of R-hadron lifetimes. They set mass limits on stop and gluino R-hadrons of 337 and 601 GeV, respectively, for lifetimes between 10 ps and 1000 seconds, and assuming direct decay to the lightest supersymmetric particle (LSP).

3.4. Searches for SUSY

Both ATLAS and CMS have updated their search for SUSY in the jets + E_T^{miss} channel [52, 53]. ATLAS explores 5 signal regions, based on differing jet multiplicities and different cuts on E_T^{miss} and H_T, the scalar sum of the E_T of the jets in the event. CMS does an analysis in the α_T variable, defined for a 2 jet topology as $\alpha_T = E_T^{jet2}/M_T$ where M_T is the transverse mass of the two jets; events with higher jet multiplicities are treated by merging the jets into two mega jets. Also of note is that ATLAS does a cut and count analysis, while CMS exploits for the first time shape information.

Backgrounds are estimated in both experiments with a mix of data-driven and Monte Carlo based methods. QCD multijet background is expected to be negligible in both experiments; background reduction is achieved through cuts on the azimuthal angle between jets and E_T^{miss}, on E_T^{miss}/H_T, and in the case of CMS, on α_T. The small QCD multijet background is confirmed in ATLAS by a dedicated study in which well-measured multijet events are smeared by jet energy response functions that have been separately measured in the data in three-jet events where two well-measured jets recoil against a third jet which points along the E_T^{miss} direction. CMS estimates W+jets background together with $t\bar{t}$ by a muon control sample, primarily selected by a requirement on M_T; the background in the signal region is estimated by scaling the number of events in the control sample by a factor determined from Monte Carlo. In the ATLAS analysis, W+jets and $t\bar{t}$ backgrounds are estimated separately, based again on a lepton control sample selected with E_T^{miss} and M_T cuts, but using a b-tag requirement (veto) to select the $t\bar{t}$ (W+jets) sample; as in the CMS analysis, extrapolation to the signal region is performed via scaling factors derived from Monte Carlo. $Z(\to \nu\overline{\nu})$+jets background is determined in both experiments via a control sample of γ+jets events; ATLAS also uses control samples of $Z(\to \ell^+\ell^-)$+jets. Background systematics are approximately comparable for the two experiments. ATLAS quotes a 50% uncertainty on $t\bar{t}$ background, but the actual level of $t\bar{t}$ background is fairly small. CMS quotes a 30% uncertainty on W+jets and $t\bar{t}$ combined, while ATLAS quotes about 25% for W+jets. For Z+jets, ATLAS has a roughly 20% uncertainty, to be compared to 40% for CMS.

In both experiments, observations are consistent with expectations from the SM. For example, Fig. 9 (left) shows the H_T distribution from CMS compared to expectations. Fig. 9 (right) shows the limits obtained by CMS in the MSUGRA/CMSSM model. The corresponding limits from ATLAS are shown in Fig. 10 (left). Both experiments are setting limits on gluino and squark masses approaching 1 TeV in certain regions of the parameter space. As shown in Fig. 10 (right) ATLAS has also updated the limits in a simplified MSSM model containing gluinos, squarks of the first and second generation and the LSP, with all other sparticles set to very

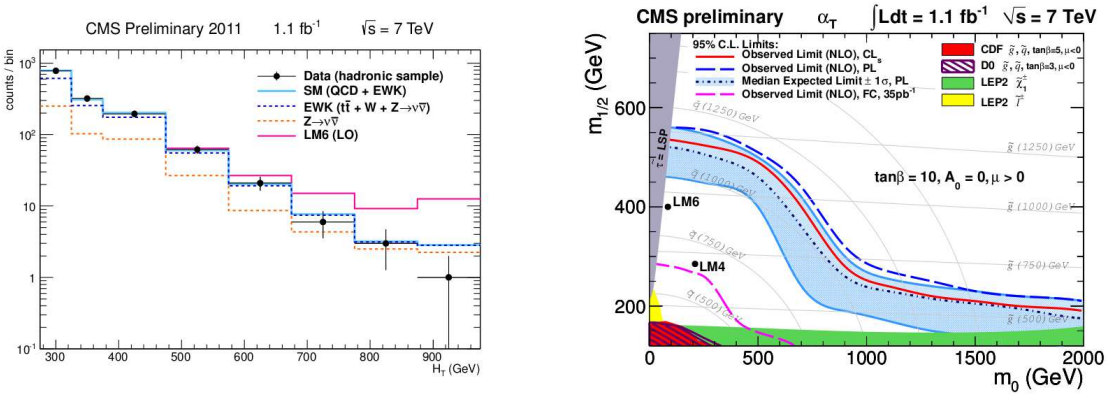


Figure 9: Left: H_T distribution from CMS the SUSY search based on the α_T variable. Right: SUSY limits in the MSUGRA/CMSSM model. From [53].

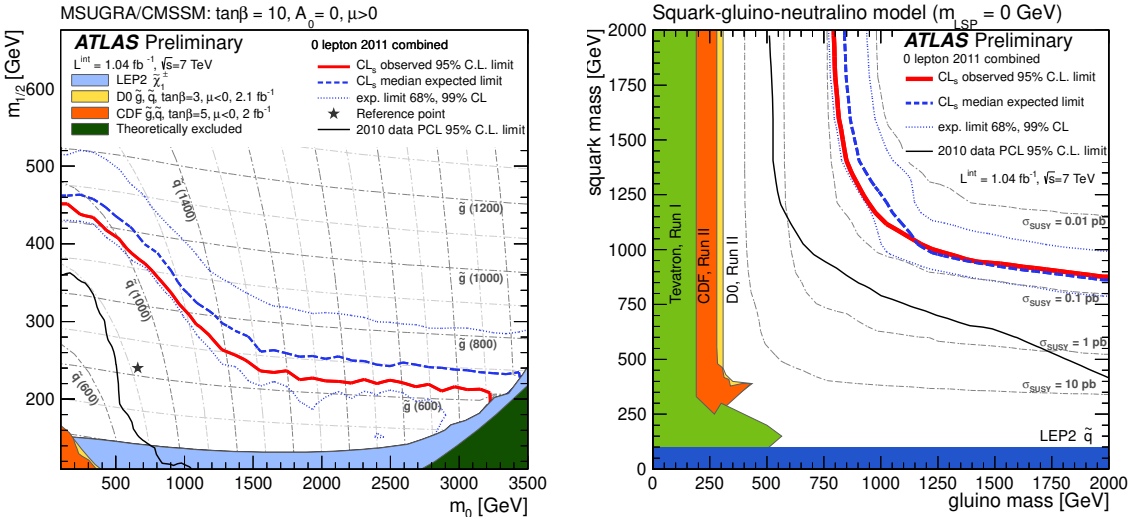


Figure 10: SUSY limits from ATLAS [52]. Left: in the MSUGRA/CMSSM model. Right: gluino and squark mass limits in a simplified MSSM model, containing only the gluino, first- and second-generation squarks and a massless LSP.

high mass. Limits approach 800 GeV for gluino masses, and are insensitive to the value of the LSP mass for LSP masses up to approximately 200 GeV.

ATLAS has updated the search in b-tagged jets plus E_T^{miss}, asking for 3 or more jets, of which one is b-tagged [54]. Four signal regions are defined, based on the number of btags versus the scalar sum of E_T^{miss} and the p_T of the jets in the event. The main background from $t\bar{t}$ is estimated from Monte Carlo. QCD multijet background is evaluated in a similar way to the ATLAS search in the jets+E_T^{miss} channel, taking into account the differences in the jet response function between light-quark and b-jets. The null search is interpreted in a simplified SUSY model containing gluinos, partners of the b quarks (sbottoms), and the LSP, with everything else set to high mass. Assuming 100% branching ratio of $\tilde{g} \to \tilde{b}_1 b$ and $\tilde{b}_1 \to b + \tilde{\chi}_1^0$, limits are set in the plane of gluino vs sbottom mass, assuming a $\tilde{\chi}_1^0$ mass of 60 GeV; the results are shown in Fig. 11 (left). Gluino masses below 720 GeV are excluded for sbottom masses up to 600 GeV. Fig. 11 (right) shows the exclusion limits that are placed in the gluino-LSP mass plane, as well as the limits on the cross section in the same plane, in a model where all the squarks are heavier than the gluino and gluino decays purely via the three-body decay $\tilde{g} \to b\bar{b}\chi_1^0$ via an off-shell sbottom.

CMS has updated the results in the dilepton + jets + E_T^{miss} channel, for both opposite-sign (OS) [55] and same-sign (SS) [56] dileptons; a new search in the Z + E_T^{miss}+jets channel has also become available [57]. In the OS search, two signal regions are defined, one with $H_T > 300$ GeV and $E_T^{miss} > 275$ GeV and the other with $E_T^{miss} > 200$ GeV and $H_T > 600$ GeV. The main background from $t\bar{t}$ is estimated using an ABCD method exploiting the lack of correlation between H_T and E_T^{miss} significance. The background estimates are

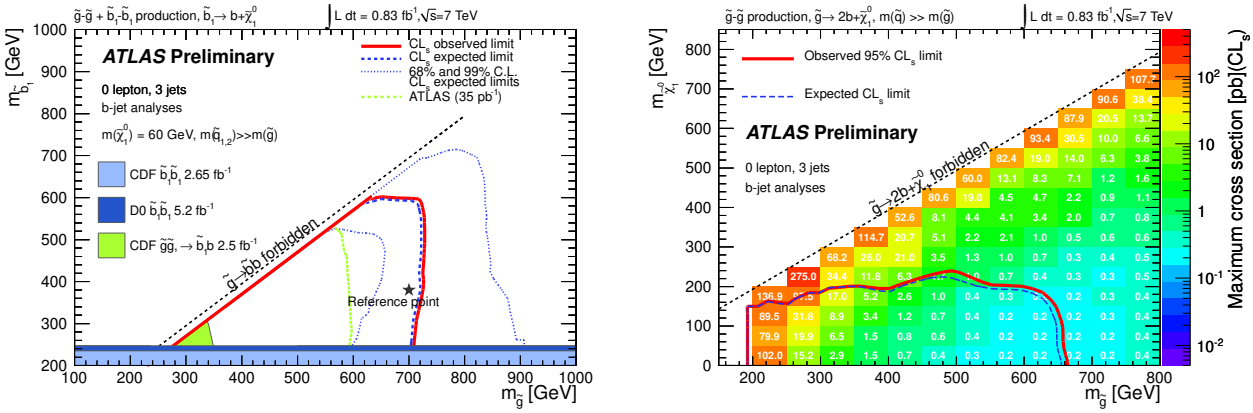


Figure 11: Left: Limits from ATLAS [54] in the gluino-sbottom mass plane, in a simplified model where $\tilde{g} \to \tilde{b}_1 b$ and $\tilde{b}_1 \to b\tilde{\chi}_1^0$. Right: Limits on the production cross section as a function of gluino and LSP mass in a model where all the squarks are heavier than the gluino and gluino decays purely via the three-body decay $\tilde{g} \to b\bar{b}\chi_1^0$ via an off-shell sbottom. The contours show the region excluded by the ATLAS analysis.

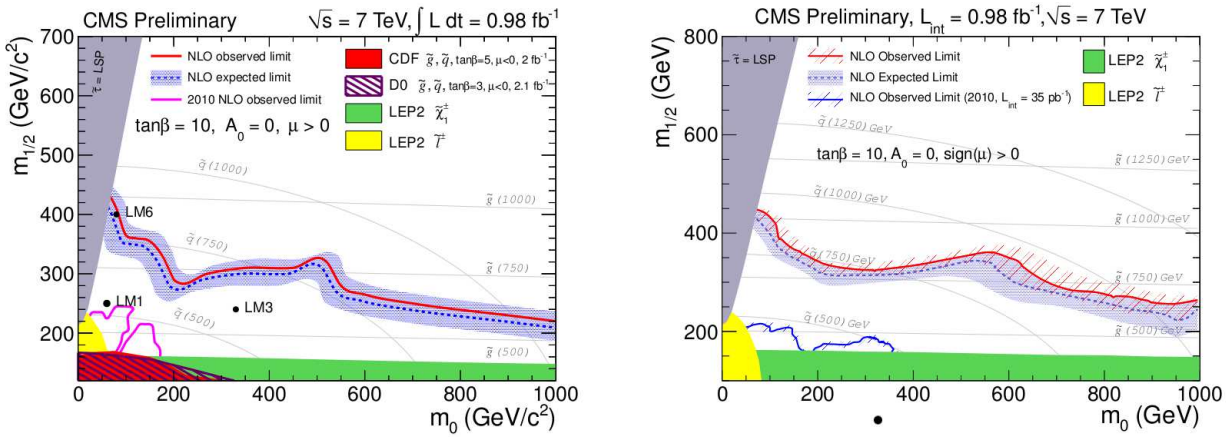


Figure 12: Limits in the MSUGRA/CMSSM model from CMS in the OS dilepton (left) [55] and SS dilepton (right) [56] channels.

cross-checked with two other methods. The first uses the observed p_T spectrum of the dilepton system to infer the p_T of the two-neutrino system from dileptonic $t\bar{t}$ decays. The second looks at the difference in the number of same-flavor versus opposite-flavor dilepton events, suitably corrected for the relative efficiency for detecting electrons versus muons. The final background estimate is taken as the uncertainty-weighted average of the two methods described above. Limits are placed in the MSUGRA/CMSSM model, and are shown in Fig. 12 (left).

The $Z + E_T^{miss}$+jets analysis requires a pair of same-flavor leptons consistent with coming from a Z, at least two jets with $p_T > 30$ GeV and $E_T^{miss} > 100$ or 200 GeV. The dominant background comes from $t\bar{t}$ and is estimated from the yield of opposite-flavor leptons, corrected for the relative efficiency for detecting electrons versus muons. The small background from Z+jets is estimated using a control sample of γ+jets events. The observed E_T^{miss} distribution is shown in Fig. 13 (left), compared to expectations. Limits are placed on a simplified model of gluino pair production with the decay $\tilde{g} \to qq\tilde{\chi}_2^0$ and $\tilde{\chi}_2^0 \to Z\tilde{\chi}_1^0$; the limit contours are shown in Fig. 13 (right). Additional information on the detector response (lepton reconstruction and isolation efficiencies, as well as the detector response for E_T^{miss}) is provided so that Monte Carlo generator-level samples can be compared to the dilepton observations.

In the same-sign dilepton search, CMS defines a number of signal regions, again based mainly on H_T and E_T^{miss}. The background from fake leptons is estimated using the standard matrix method. Via the use of a hadronic trigger, regions of low lepton p_T can be probed. Taus are also included in the analysis. Limits are placed in the MSUGRA/CMSSM model here as well, as shown in Fig. 12 (right). In addition, simple parametrizations of the detector efficiency and resolution are provided, allowing comparison of a variety of Monte Carlo models with the experimental results.

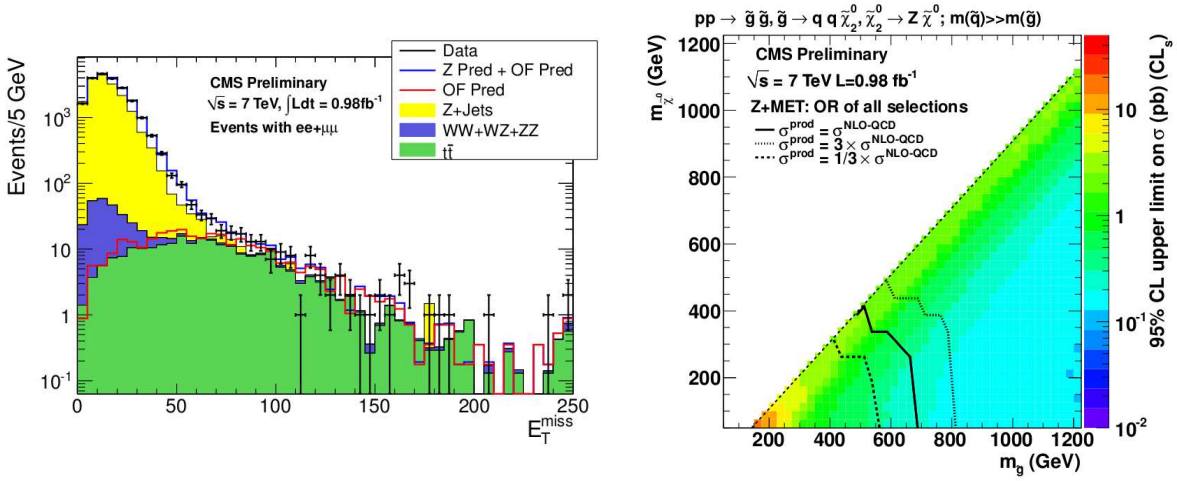


Figure 13: Left: observed E_T^{miss} distribution from the CMS $Z + E_T^{miss}$+jets analysis [57]. Right: Cross section limits in the gluino-LSP plane, assuming a simplified model of gluino pair production, followed by the decay $\tilde{g} \to qq\tilde{\chi}_2^0$ and $\tilde{\chi}_2^0 \to Z\tilde{\chi}_1^0$.

3.5. Outlook

By the end of 2011, ATLAS and CMS are expected to have accumulated approximately 4-5 fb^{-1} of data. The 2012 run could extend this to about 10 fb^{-1} per experiment. BSM searches will continue to push out to higher mass, but with steeply falling cross sections, significant gains in mass reach will be hard to come by. More significant gains might be expected by pushing towards smaller couplings, or in the case of SUSY, gaining access to new production processes. SUSY searches at the LHC have so far concentrated on strong production of gluinos and squarks of the first and second generations. With higher integrated luminosities, direct production of third generation squarks and direct gaugino production should become accessible. It should be noted that the Tevatron experiments still have the best limits on stop [13, 58], sbottom [59], and gaugino [60] production. Even direct slepton production might be detectable. Another priority is to extend the SUSY searches to more challenging decay chains, those with small mass differences in the decay cascade, or conversely highly boosted LSP's.

4. Conclusion

A very rich program of BSM searches continues at CDF and D0, with typically 5-6 fb^{-1} analyzed to this point, out of 11.5 fb^{-1} delivered. Best limits on new physics are still coming from the Tevatron in a number of cases. The attention of the community has focused on a few recent anomalies from the Tevatron. Whether these are "mirages" or signs of new physics remains to be seen; the analyses are being followed up with the full dataset. Crosschecks by the LHC experiments will provide further information.

At the LHC, as of the end of July, ATLAS and CMS are starting to produce results with 1 fb^{-1} of data analyzed. Both experiments are exploring a wide variety of signatures and trying out new ways to present their results in as model-independent manner as possible. There is unfortunately no sign of new physics yet from the LHC.

Returning to the desert theme that opened this note, one of the most famous desert stories in the Western canon is the biblical story in Exodus in which Moses finally catches a glimpse of the Promised Land after 40 years of wandering in the desert. In this context, perhaps it is worth recalling that this year marks the 40th year since the birth of SUSY [61] and the 37th anniversary[3] of the "November revolution" [62, 63]. Long ago,

[3] To first order, 40 years.

the wise ones in our field promised the "LHC no lose theorem". It can only be hoped that this is the year in which the Promise is realized.[4]

References

1 R.Park, "Large Hadron Collider: no big surprises at the half-energy point", *What's New*, July 29, 2011. http://www.bobpark.org
2 CDF: http://www-cdf.fnal.gov/physics/exotic/exotic.html,
D0: http://www-d0.fnal.gov/Run2Physics/WWW/results/np.htm,
ATLAS Exotics: https://twiki.cern.ch/twiki/bin/view/AtlasPublic/ExoticsPublicResults,
ATLAS SUSY: https://twiki.cern.ch/twiki/bin/view/AtlasPublic/SupersymmetryPublicResults,
CMS Exotics: https://twiki.cern.ch/twiki/bin/view/CMSPublic/PhysicsResultsEXO,
CMS SUSY: https://twiki.cern.ch/twiki/bin/view/CMSPublic/PhysicsResultsSUS
3 S.Stone, these proceedings.
4 K.Tollefson, these proceedings.
5 CDF Collaboration, CDF Public Note 10479.
6 D0 Collaboration, in preparation.
7 D0 Collaboration, arXiv:1106.6308 [hep-ex].
8 D0 Collaboration, *Phys. Lett.* **B699** (2011) 145.
9 D0 Collaboration, *Phys. Rev. Lett.* **107** (2011) 011801.
10 D0 Collaboration, arXiv:1107.1849 [hep-ex].
11 D0 Collaboration, arXiv:1104.4522 [hep-ex].
12 D0 Collaboration, *Phys. Rev. Lett.* **105** (2010) 221802.
13 D0 Collaboration, *Phys. Lett.* **B696** (2011) 321.
14 CDF Collaboration, CDF note 10479.
15 CDF Collaboration, CDF note 10603.
16 CDF Collaboration, CDF note 10270.
17 CDF Collaboration, *Phys. Rev. Lett.* **107** (2011) 042001.
18 CDF Collaboration, arXiv:1107.3875 [hep-ex].
19 CDF Collaboration, arXiv:1101.5728 [hep-ex].
20 CDF Collaboration, arXiv:1107.3574 [hep-ex].
21 CDF Collaboration, CDF note 10468.
22 CDF Collaboration, CDF note 10539.
23 CDF Collaboration, CDF note 10464.
24 CDF Collaboration, arXiv:1106.4782 [hep-ex].
25 CDF Collaboration, *Phys. Rev. Lett.* **106** (2011) 171801, arXiv:1104.0699 [hep-ex].
26 http://www-cdf.fnal.gov/physics/ewk/2011/wjj/7_3.html
27 D0 Collaboration, *Phys. Rev. Lett.* **107** (2011) 011804.
28 ATLAS Collaboration, ATLAS-CONF-2011-097.
29 CDF Collaboration, *Phys. Rev.* **D83** (2011) 112003.
30 J.M.Campbell, R.K.Ellis and D.L.Rainwater, *Phys. Rev.* **D68** (2003) 094021.
31 CDF Collaboration, CDF Public Note 10436.
32 D0 Collaboration, arXiv:1107.4995 [hep-ex].
33 ATLAS Collaboration, ATLAS-CONF-2011-106.
34 CMS Collaboration, CMS-PAS-TOP-11-014.
35 ATLAS Collaboration, arXiv:1108.1582 [hep-ex].
36 CMS Collaboration, CMS-PAS-EX0-11-019.
37 ATLAS Collaboration, arXiv:1108.1316 [hep-ex].
38 CMS Collaboration, CMS-PAS-EXO-11-024.
39 ATLAS Collaboration, ATLAS-CONF-2011-109.
40 D0 Collaboration, *Phys. Rev. Lett.* **105** (2010) 191802.

[4] But if we insist on 40 years since the "November revolution" this would imply having to wait for 14 TeV running at the LHC!

41 M.Cacciari, G.P.Salam and G.Soyez, *JHEP* **04** (2008) 063,
M.Cacciari and G.P.Salam, *Phys. Lett.* **B641** (2006) 57.
42 ATLAS Collaboration, arXiv:1108.6311 [hep-ex].
43 CMS Collaboration, arXiv:1107.4771 [hep-ex].
44 CMS Collaboration, CMS-PAS-EXO-11-006.
45 CMS Collaboration, CMS-PAS-EXO-11-051.
46 ATLAS Collaboration, ATLAS-CONF-2011-096.
47 CMS Collaboration, CMS-PAS-EXO-11-071.
48 D.-C. Gai, G.Starkman, D.Stojkovic *et al.*, *Phys. Rev.* **D77** (2008) 076007.
49 CMS Collaboration, CMS-PAS-EXO-11-022.
50 B.C.Allanach *et al. Eur. Phys. J.* **C25** (2002) 113.
51 CMS Collaboration, CMS-PAS-EXO-11-020.
52 ATLAS Collaboration, arXiv:1109.6572 [hep-ex].
53 CMS Collaboration, arXiv:1109.2352 [hep-ex].
54 ATLAS Collaboration, ATLAS-CONF-2011-098.
55 CMS Collaboration, CMS-PAS-SUS-11-011.
56 CMS Collaboration, CMS-PAS-SUS-11-010.
57 CMS Collaboration, CMS-PAS-SUS-11-017.
58 CDF Collaboration, *Phys. Rev. Lett.* **104** (2010) 251801.
59 D0 Collaboration, *Phys. Lett.* **B693** (2010) 95.
60 D0 Collaboration, *Phys. Lett.* **B680** (2009) 34.
61 Y.A.Golfand and E.P.Likhtman, *JETP Lett.* **13** (1971) 323.
62 J.Aubert *et al.*, *Phys. Rev. Lett.* **33** (1974) 1404.
63 J.Augustin *et al.*, *Phys. Rev. Lett.* **33** (1974) 1406.